Published in final edited form as:

Science. 2019 November 15; 366(6467): 838–843. doi:10.1126/science.aay0033.

Structure of the RSC complex bound to the nucleosome

Youpi Ye[1,2,*], **Hao Wu**[2,3,*], **Kangjing Chen**[1,2], **Cedric R. Clapier**[4], **Naveen Verma**[4], **Wenhao Zhang**[2], **Haiteng Deng**[2], **Bradley R. Cairns**[4,7], **Ning Gao**[5,7], **Zhucheng Chen**[1,2,6,7]

[1]MOE Key Laboratory of Protein Science, Tsinghua University, Beijing, 100084, P.R. China

[2]School of Life Science, Tsinghua University, Beijing, 100084, P.R. China

[3]Peking University–Tsinghua University–National Institute of Biological Sciences Joint Graduate Program, Beijing 100084, China

[4]Howard Hughes Medical Institute and Department of Oncological Sciences, Huntsman Cancer Institute, University of Utah School of Medicine, Salt Lake City UT, 84112

[5]State Key Laboratory of Membrane Biology, Peking-Tsinghua Joint Center for Life Sciences, School of Life Sciences, Peking University, Beijing 100871

[6]Tsinghua-Peking Joint Center for Life Sciences, Beijing Advanced Innovation Center for Structural Biology, Beijing 100084, China

Abstract

The RSC complex remodels chromatin structure and regulates gene transcription. We report the cryoEM structure of yeast RSC bound to the nucleosome. RSC is delineated into the ATPase motor, the actin-related-protein (ARP) module, and the substrate-recruitment module (SRM). RSC binds the nucleosome mainly through the motor, with the auxiliary subunit Sfh1 engaging the H2A-H2B acidic patch to enable nucleosome ejection. SRM is organized into three substrate-binding lobes poised to bind their respective nucleosomal epitopes. The relative orientations of the SRM and the motor on the nucleosome explain the directionality of DNA translocation and promoter nucleosome repositioning by RSC. Together, our findings shed light on RSC assembly and functionality, and provide a framework to understand the mammalian homologs BAF/PBAF and the Sfh1 ortholog INI1/BAF47, which are frequently mutated in cancers.

In chromatin, DNA wraps around histone octamers to form nucleosomes. Access to the nucleosomal DNA is facilitated by Snf2-family chromatin remodelers, which are highly conserved from yeast to mammals(1). Snf2 and Sth1, two closely related paralogs, are the catalytic motor subunits of the two similar yeast SWI/SNF and RSC remodeling complexes,

[7]Correspondence to zhucheng_chen@tsinghua.edu.cn; gaon@pku.edu.cn; Brad.Cairns@hci.utah.edu.
[*]These authors make equal contribution to this work

Author contributions: Y.Y. prepared the samples for EM and MS analyses; W.Z, K.C. H.D. performed MS analyses; H.W. K.C., N.G., and Z.C. performed EM analysis and model building; C.C., N.V., and B.C. conducted genetic and biochemical analyses. Z.C. oversaw the project, and wrote the manuscript with help from all the authors.

Competing interests: Authors declare no competing interests.

Data and materials availability: Density maps are deposited at the Electron Microscopy Database (accession code EMD-9905, 0777, 0778) and protein coordinates are deposited at the Protein Data Bank (PDB 6K15, 6KW3, and 6KW4) for the SRM, Class A complex and Class B complex, respectively.

respectively. Although the motors remodel nucleosomes *in vitro* on their own, they function in complexes with multiple auxiliary subunits *in vivo* to provide regulation and targeting. RSC is enriched at nucleosomes that flank nucleosome free regions (NFRs), and controls the promoter architecture of most genes in yeast (2). It employs DNA translocation to slide or eject the promoter +1 nucleosomes to extend NFRs, possibly to expose transcription start sites and promote transcription.

Low-resolution structures of the SWI/SNF, RSC and the human homolog PBAF complexes have been reported(3, 4). However, how the subunits assemble the complexes and engage nucleosomes remain unclear. Here we reported the cryo-electron microscopy (cryoEM) structure of RSC bound to the nucleosome, providing insights into RSC organization and function.

Overall structure of RSC bound to the nucleosome

Purified RSC was mixed with nucleosomes and the stable ATP analog ADP-BeF_x, and subjected to cryoEM analysis (Fig. S1 and Table S1). The RSC-nucleosome complexes were highly flexible, with two prominent classes identified. One class (Class A) showed a slightly unwrapped linker DNA, with an overall resolution of 7.1 Å (Fig. S2A and S2B), whereas the other class (Class B) showed EM density for a longer linker DNA, with an overall resolution of 7.6 Å (Fig. S2C–S2E). RSC in either class was organized into three modules (Fig. 1A and Movie S1): the motor module (motor domain of Sth1), the ARP module (the HSA helix of Sth1 bound by an Arp7-Arp9-Rtt102 trimer), and the substrate-recruitment module (SRM, including the N-terminal fragment of Sth1 and multiple additional subunits). The three modules, connected through two disordered loops of Sth1, showed rigid-body motions relative to each other (Fig. S3), explaining the flexibility. Since the biological implications of Classes A and B were the same, we mainly focused on the 7.1 Å Class A structure.

Focused refinements led to a 3.8 Å map of the motor domain (Fig. S2F), and a 3.4 Å map of the SRM, with the rigid core at ~ 3.0 Å (Figs. S1G and S2G–S2K). The high-quality map of SRM allowed us to build atomic models of the N-terminal fragments of Sth1, Rsc2, Rsc3, Rsc4, Rsc6, Rsc7, Rsc9, Rsc30, Rsc58, Htl1, Sfh1 and two molecules of Rsc8 (termed Rsc8a and Rsc8b) (Fig. 1B). The interactions between the subunits were further validated by crosslinking mass-spectrometry (CL-MS) analyses (Fig. S4 and Suppl. Dataset 1).

The nucleosome is mainly bound by the motor domain of Sth1, with limited contacts from other subunits, except Sfh1 (see below). An open space is embraced by the SRM and some weak density was found (Fig. S2B and S2D), which may relate to the hypothetical nucleosome-binding central cavity proposed previously(5). However, no nucleosome was found inside this open space.

The SRM comprises the majority of RSC (Fig. 1A), with the conserved subunits Rsc6, Rsc8, Rsc9, Rsc58 and the N-terminal fragment of Sth1, interweaving into a rigid core. The SRM is further organized into three lobes. Rsc3 and Rsc30, which contain DNA-binding Zn-cluster domains (ZnDs), decorate the conserved core at DNA-binding lobe (DB-lobe) (6, 7). Rsc2 and Rsc4, which contain histone-tail binding bromodomains (BDs) and BAH

domain (8–10), are located at the histone-tail binding lobe (HB-lobe). Sfh1, which contains a nucleosome-binding C-terminal tail (CTT, discussed below), is located at the nucleosome-binding lobe (NB-lobe). Due to tethering to the SRM through flexible loops, the structures of the substrate-binding motifs (e.g. ZnD, BD, BAH and CTT) could not be resolved under current conditions. Nevertheless, the SRM clearly positions these elements to colocalize along one side of the nucleosome, with the DB, HB and NB-lobes proximal to their binding epitopes, suggesting mechanisms for coordinated nucleosome recruitment or retention.

Structure of Sth1 in the context of the RSC complex

Sth1 is composed of five major domains (Figs. 1B and 2A): the N-terminal domain (NTD), the domain preceding the HSA-helix (preHSA), HSA, motor, and the C-terminal extension and BD. A poly-alanine model was built for the poorly conserved NTD because of the lack of defined features (Fig. S5A). The modestly conserved preHSA (~25% identity between Sth1 and HsBRG1) threads through the DB and HB- lobes. The HSA helix connects to the preHSA and motor domains through flexible loops. The motor domain interacts with the nucleosome in a manner very similar to the isolated ATPase fragment of Snf2 (Fig. S6) (11, 12).

One surface of HSA binds to the ARP proteins as observed in the structure of HSA^{Snf2}(13), and the exposed surface, containing multiple conserved positively charged residues (Fig. S5A), is proximal to the nucleosomal DNA (Figs. 2A and S5B). The structure suggests that HSA may function to orient RSC by projecting the ARP proteins away from the nucleosome, and orienting HSA, the preHSA and the associated SRM towards the exit DNA (Fig. 2A). As a result, we found one preferred nucleosome orientation with the linker DNA at the exit side. This contrasts with the isolated motor domain of Snf2, which binds to either of the two nucleosome orientations in the presence of ADP-BeF_x(11).

The ARP proteins adopt a conformation largely similar to that found in the crystal structure of the HSA^{Snf2}-Arp7-Arp9-Rtt102 complex, and make limited direct interaction with the nucleosome or the Sth1 motor domain. The structure suggests that the ARPs may stabilize the helical conformations of HSA and/or affect the conformation of the adjacent post-HSA, which interacts with the motor (14, 15), and hence modulate the structural integrity of the complex and the remodeling efficiency(16).

The preHSA interacts with several conserved auxiliary subunits (Fig. 2B). Specifically, Arg292 of Sth1 packs against Rsc9 at the DB-lobe (Figs. S5C and S2I). Likewise, Arg258, Arg198 and Arg202 interact with Rsc8 and Rsc58 at the HB-lobe (Fig. S5D–S5E). These residues are highly conserved (Fig. S5A), with mutations of the equivalent residues recurrently found in human cancers (17).

Structure of the NB-lobe and the implication in nucleosome binding

Sfh1 is a major component of the NB-lobe (Fig. 3A). It is highly conserved with Snf5 in budding yeast and INI1/BAF47 in animals (Fig. S7A). The conserved domain contains two imperfect repeats, Repeat 1 (RPT1) and Repeat 2 (RPT2), which interact with the SWIRM domains of Rsc8a and Rsc8b, respectively (Figs. 3B and S2H). This is in line with

the crystal structure of RPT1 domain of INI1 bound to the SWIRM domain of BAF155 (homolog of Rsc8) (18). The INI1-BAF155 interaction is highly similar to that of Sfh1-Rsc8 (Fig. S7B), supporting a conserved assembly mechanism.

One prominent feature of the NB-lobe is the CTT of Sfh1, which is close to the H2A-H2B dimer and the H4 tail of the nucleosome but largely disordered in the structure (Fig. 3C). The CTTs of Sfh1 homologs are enriched in positively charged residues (Fig. 3D), suggesting that these residues may bind to the acidic pocket of H2A-H2B, and/or the nearby DNA strands. In line with this idea, a block of EM density proximal to the CTT was identified above the H2A-H2B surface (Fig. S8A). Similar to Snf5 (19, 20), the CTT of Sfh1 crosslinks to H2A and H2B (Fig. S4B), supporting close proximity in space.

Regarding CTT function, whereas a plasmid encoding WT *SFH1* fully complemented the lethal phenotype of *sfh1Δ* (21), a plasmid encoding the *sfh1* CTT truncation mutant (aa 1–384, named Sfh1-ΔCTT) restored viability, but displayed multiple strong conditional phenotypes, likely resulting from defects in the transcription of stress response genes (22)(Figs. 3E and S8B). Furthermore, the loss of individual arginine or lysine residues (replacement by alanine) in the CTT did not confer phenotypes, suggesting the functional involvement of multiple positively charged residues. To further explore the function of the CTT, we examined its nucleosome binding *in vitro* (Fig. S8C and S8D). The CTT bound the nucleosome, and mutation of the individual conserved positively charged residues R401A, R404A, K403A or R400A, modestly weakened the binding. Interestingly, mutations of all four residues together largely diminished the binding, suggesting the CTT may bind to the nucleosome through multivalent interactions.

To determine the role of the Sfh1 CTT in nucleosome remodeling, we purified (Fig. S8E) and compared the biochemical activity of WT to mutant RSC lacking the Sfh1 CTT (Sfh1-ΔCTT). The nucleosome-dependent ATPase activity and the nucleosome sliding activity (on yeast *5S* nucleosomes) of the mutant complex were robust and comparable to WT (Figs. 3F and S8F). Notably, RSC Sfh1-ΔCTT was unable to eject yeast nucleosomes residing in closed circular arrays, whereas WT RSC was fully capable of ejection (Fig. 3G). These results suggested that the Sfh1 CTT helps RSC bind to the dish face of the nucleosome and stabilize RSC association during DNA translocation, enabling nucleosome ejection (16, 23, 24). Taken together, the CTT of Sfh1, by homology INI1/BAF47 in human cells, functioned to stably anchor RSC on the nucleosome, facilitating nucleosome ejection *in vitro* and fitness *in vivo*.

The NB-lobe contains one additional component, Rsc7. Whereas the N-terminal region of the Rsc7 is not essential for the RSC assembly, the C-terminal domain (CTD) confers full Rsc7 function (22). Consistent with these studies, the NTD could not be detected in the structure, whereas the CTD was identified (Fig. S9A), which staples Sfh1 and Rsc8b together (Fig. 3H). The Sfh1-Rsc8-binding sequence of Rsc7 is conserved in animal BAF45a (α1, Fig. S10). In agreement, BAF45a crosslinks to the Sfh1 homolog in the PBAF complex(25).

Structure of the DB-lobe and the implications in exit DNA binding

The core of the DB-lobe is comprised of Rsc9, Rsc6, the coiled-coil (CC) domain of Rsc8, the C-terminal half of preHSA, and a middle segment of Rsc58 (Fig. 4A). On the surface of the DB-lobe reside the yeast-specific subunits, Rsc3, Rsc30 and Htl1 (Fig. 4A).

Rsc9 is composed of armadillo repeats (Fig. S11A)(26), referred as the Rsc9 homology domain (R9HD). The R9HD binds to Rsc6 and preHSA at the DB-lobe, with the less conserved N-terminal tail extending to the HB-lobe (Fig. S9B). The R9HD shows some conservation to BAF200 in animals, with ~30% sequence similarity to human BAF200 (Fig. S11B), which is the characteristic component of the PBAF complex(1).

Rsc8 is a multi-domain protein, containing SWIRM, zinc finger (ZnF), SANT and CC domains (Fig. 4B). All these structural elements except ZnF domain are highly conserved (Fig. S12). Consistent with a previous study(27), Rsc8a and Rsc8b dimerize mainly through the CC domains. The Rsc8 dimer connects the three lobes of SRM together, with SWIRM at the NB-lobe, ZnF and SANT at the HB-lobe, and CC at the DB-lobe (Figs. 4C and S9C), suggesting a key role of Rsc8 in RSC assembly. These findings provide the structural basis for the earlier studies suggesting the formation of a core complex by BRG1-BAF155-BAF170-INI1 tetramer (28), and the central role of BAF155-BAF170 in the BAF/PBAF assembly (25).

Rsc6, which is highly similar to Swp73 in yeast and BAF60s in animals (Fig. S13A), bundles to the CC domain of Rsc8 (Figs. 4A and S9D). In support of the conservation, the SWIB domain of Rsc6 adopts a structure homologous to that of mouse BAF60a (Fig. S13B). The domain following SWIB extends out from the DB-lobe and does not fold into a rigid conformation, contacting the weak EM density that probably results from Rsc3 and Rsc30 (Fig. S2B and S2D). We speculate that Swp73 and BAF60s may fold into the same structure as Rsc6, with a domain extending to bind to different transcription factors (29, 30), supporting the function of the DB-lobe in linker DNA binding.

The middle Rsc6-binding domain (R6BD) of Rsc58 binds to Rsc6 and Rsc8 (Fig. S14B). The interacting residues are highly conserved (Figs. S11–S14), suggesting this structure may serve as a model for the human complexes. In support of this notion, the Rsc58 homolog BRD7 is a unique component of the PBAF complex (25, 31).

Rsc3 and Rsc30 are yeast-specific transcription factors, which can heterodimerize and show a binding preference for GC-rich DNA sequences (6, 7, 32). Rsc3 and Rsc30 each contains an N-terminal DNA-binding ZnD, a dimerization domain (DD) and a CTD (Fig. 1B). Short β-sheets and helices of the DDs were identified forming a dimer binding to the surface of Rsc9 (Fig. 4A). The interaction between the dimerization helices was also detected by the CL-MS analysis (Fig. S4B). Weak EM densities near the DDs were found (Fig. S2E), which may result from the flexible ZnDs and CTDs of Rsc3 and Rsc30.

The DDs of Rsc3 and Rsc30 are located on the DB-lobe at a position distal to the DNA entry side, but close to the exit side, and thus position the N-terminal ZnDs to bind the exit DNA (Fig. 4D). The N-termini of DDs are ~60 Å away from the exit DNA, and connect to the

ZnDs through spacer sequences with a length of ~100 residues, which would allow a large degree of flexibility to sample the exit DNA. Htl1, a yeast-specific small subunit of RSC, binds to CC of Rsc8 (Fig. 4A and S9F), in agreement with interactions between Htl1 and the C-terminus of Rsc8(33).

Structure of the HB-lobe and the implication in histone tail binding

RSC and PBAF both contain subunits carrying multiple BDs, such as Rsc2 and Rsc4 in RSC, and their ortholog BAF180 in PBAF, which are partly responsible for recruitment of the complexes through binding to histone tails(8, 10). Interestingly, these histone tail-binding elements cluster at the HB-lobe (Fig. 4E), containing one additional histone-tail binding element, the BD of Rsc58 (Fig. 4F).

Whereas the structures of the BDs and BAH of Rsc2 and Rsc4 could not be detected, the CTDs of Rsc2 (residues 741–883) and Rsc4 (residues 364–625) were identified, which map to the tip of the HB-lobe (Fig. 4E). This structure is consistent with the studies showing that the CTD of Rsc2 is necessary and sufficient for RSC assembly(34). Similarly, the C-terminus of Rsc4 mediates RSC assembly (8). The CTDs of Rsc2 and Rsc4 are exposed at the surface, and ~70 Å away from the H3 tails. They connect to the N-terminal BAH and BDs through long spacer sequences with a length of over 100 and 50 residues, respectively, which would poise these histone-tail binding elements to access their substrates, in agreement with the functions of BDs and BAH in histone-tail binding(9, 10). The BD of Rsc58 loosely pack at the periphery of the HB-lobe (Fig. 4F), with its histone-binding pocket exposed to solvent and ~60 Å away from histone H3 (Class B complex, Fig. S3A), suggesting Rsc58 might still bind to the histone H3 tails. The spatial proximity of the BDs and BAH domains to the histone tails was also supported by the CL-MS analysis (Fig. S4B).

Discussion

In this work, we determined the structure of RSC bound to the nucleosome. Within RSC, Sth1 functions as a global organizer orchestrating the complex into three modules (Fig. 5A), and Rsc8 works as a local organizer delineating the SRM into three substrate-binding lobes (Fig. 5B).

RSC binds to the nucleosome primarily through the motor domain of Sth1, with the majority of the histone-DNA contacts maintained. This model is different from the previous notion of nucleosome embracement (5), which was proposed to result in extensive rearrangement of histone-DNA contacts to facilitate DNA translocation. Our findings support a unified mechanism of chromatin that involves the action of the motor domain itself(12, 35). This is consistent with DNA translocation by the different remodelers involving 1–2 bp movements of DNA along the octamer surface(11, 24, 36–38).

RSC repositions the promoter +1 nucleosome away from the NFR, whereas ISWI slides the nucleosome towards the open DNA (39, 40). Our structure suggested that Rsc3-Rsc30 bind to the open NFR DNA such that the motor of Sth1 is loaded onto the +1 nucleosome at the side distal to the NFR (Fig. 5A). RSC would then push the +1 nucleosome away from the

NFR. In contrast, the HSS domain of ISWI binds to the NFR DNA, and positions the motor domain to the nucleosome at the proximal side, and thus slides the nucleosome towards the NFR (39). Therefore, Rsc3/30 in RSC and HSS in ISWI both recognize the NFR DNA, yet the specific architectures of these remodeling complexes position their motors differently, enabling the enzymes to respond to the chromatin cues distinctly, and conferring specific functions at promoters.

The structure of RSC also sheds light on the assembly of the mammalian homologs PBAF and BAF. In addition to the well-known conserved components (1), our work provided evidence that yeast Rsc2 and Rsc4 together represent the mammalian polybromo protein BAF180, as Rsc2 and Rsc4 are adjacent, and their BAH and BDs combine to largely constitute polybromo. Furthermore, we showed that BAF45a, BAF200 and BRD7, which are the characteristic subunits of the PBAF(25), are homologous to Rsc7, Rsc9 and Rsc58 in RSC, respectively.

Supplementary Material

Refer to Web version on PubMed Central for supplementary material.

Acknowledgements

We thank the Electron Microscopy Laboratory, CryoEM platform, and High-performance Computing Platform of Peking University, and the Bio-Computing Platform at Tsinghua University.

Funding: the National Key Research and Development Program (2017YFA0102900 to Z.C., 2016YFA0500700 to N.G.), the National Natural Science Foundation of China (31570731 and 31630046 to Z.C., 31725007 and 31630087 to N.G.), HHMI (B.C.), NCI R01 CA 201396 (C.C. and N.V.), and NCI CA042014 to Huntsman Cancer Institute for core facilities.

References and Notes

1. Clapier CR, Cairns BR, The biology of chromatin remodeling complexes. Annu. Rev. Biochem78, 273 (2009). [PubMed: 19355820]
2. Lorch Y, Kornberg RD, Chromatin-remodeling for transcription. Q. Rev. Biophys50, e5 (2017). [PubMed: 29233217]
3. Leschziner AE, Electron microscopy studies of nucleosome remodelers. Curr. Opin. Struct. Biol21, 709 (2011). [PubMed: 22040801]
4. Zhang Zet al., Architecture of SWI/SNF chromatin remodeling complex. Protein Cell9, 1045 (2018). [PubMed: 29546678]
5. Chaban Yet al., Structure of a RSC-nucleosome complex and insights into chromatin remodeling. Nat. Struct. Mol. Biol15, 1272 (2008). [PubMed: 19029894]
6. Angus-Hill MLet al., A Rsc3/Rsc30 zinc cluster dimer reveals novel roles for the chromatin remodeler RSC in gene expression and cell cycle control. Mol. Cell7, 741 (2001). [PubMed: 11336698]
7. Badis Get al., A library of yeast transcription factor motifs reveals a widespread function for Rsc3 in targeting nucleosome exclusion at promoters. Mol. Cell32, 878 (2008). [PubMed: 19111667]
8. Kasten Met al., Tandem bromodomains in the chromatin remodeler RSC recognize acetylated histone H3 Lys14. EMBO J. 23, 1348 (2004). [PubMed: 15014446]
9. Chambers AL, Pearl LH, Oliver AW, Downs JA, The BAH domain of Rsc2 is a histone H3 binding domain. Nucleic Acids Res. 41, 9168 (2013). [PubMed: 23907388]
10. VanDemark APet al., Autoregulation of the rsc4 tandem bromodomain by gcn5 acetylation. Mol. Cell27, 817 (2007). [PubMed: 17803945]

11. Li Met al., Mechanism of DNA translocation underlying chromatin remodelling by Snf2. Nature567, 409 (2019). [PubMed: 30867599]
12. Clapier CR, Iwasa J, Cairns BR, Peterson CL, Mechanisms of action and regulation of ATP-dependent chromatin-remodelling complexes. Nat. Rev. Mol. Cell Biol18, 407 (2017). [PubMed: 28512350]
13. Schubert HLet al., Structure of an actin-related subcomplex of the SWI/SNF chromatin remodeler. Proc. Natl. Acad. Sci. U S A110, 3345 (2013). [PubMed: 23401505]
14. Liu X, Li M, Xia X, Li X, Chen Z, Mechanism of chromatin remodelling revealed by the Snf2-nucleosome structure. Nature544, 440 (2017). [PubMed: 28424519]
15. Xia X, Liu X, Li T, Fang X, Chen Z, Structure of chromatin remodeler Swi2/Snf2 in the resting state. Nat. Struct. Mol. Biol, (2016).
16. Clapier CRet al., Regulation of DNA Translocation Efficiency within the Chromatin Remodeler RSC/Sth1 Potentiates Nucleosome Sliding and Ejection. Mol. Cell62, 453 (2016). [PubMed: 27153540]
17. Gao Jet al., Integrative analysis of complex cancer genomics and clinical profiles using the cBioPortal. Sci. Signal6, pl1 (2013). [PubMed: 23550210]
18. Yan L, Xie S, Du Y, Qian C, Structural Insights into BAF47 and BAF155 Complex Formation. J. Mol. Biol429, 1650 (2017). [PubMed: 28438634]
19. Dechassa MLet al., Architecture of the SWI/SNF-nucleosome complex. Mol. Cell Biol28, 6010 (2008). [PubMed: 18644858]
20. Sen Pet al., Loss of Snf5 Induces Formation of an Aberrant SWI/SNF Complex. Cell Rep. 18, 2135 (2017). [PubMed: 28249160]
21. Cao Y, Cairns BR, Kornberg RD, Laurent BC, Sfh1p, a component of a novel chromatin-remodeling complex, is required for cell cycle progression. Mol. Cell Biol17, 3323 (1997). [PubMed: 9154831]
22. Wilson B, Erdjument-Bromage H, Tempst P, Cairns BR, The RSC chromatin remodeling complex bears an essential fungal-specific protein module with broad functional roles. Genetics172, 795 (2006). [PubMed: 16204215]
23. Dechassa MLet al., SWI/SNF has intrinsic nucleosome disassembly activity that is dependent on adjacent nucleosomes. Mol. Cell38, 590 (2010). [PubMed: 20513433]
24. Sirinakis Get al., The RSC chromatin remodelling ATPase translocates DNA with high force and small step size. EMBO J30, 2364 (2011). [PubMed: 21552204]
25. Mashtalir Net al., Modular Organization and Assembly of SWI/SNF Family Chromatin Remodeling Complexes. Cell175, 1272 (2018). [PubMed: 30343899]
26. Reichen Cet al., Structures of designed armadillo-repeat proteins show propagation of inter-repeat interface effects. Acta Crystallogr. D Struct. Biol72, 168 (2016). [PubMed: 26894544]
27. Treich I, Carlson M, Interaction of a Swi3 homolog with Sth1 provides evidence for a Swi/Snf-related complex with an essential function in Saccharomyces cerevisiae. Mol. Cell Biol17, 1768 (1997). [PubMed: 9121424]
28. Phelan ML, Sif S, Narlikar GJ, Kingston RE, Reconstitution of a core chromatin remodeling complex from SWI/SNF subunits. Mol. Cell3, 247 (1999). [PubMed: 10078207]
29. Wang RRet al., The SWI/SNF chromatin-remodeling factors BAF60a, b, and c in nutrient signaling and metabolic control. Protein Cell9, 207 (2018). [PubMed: 28688083]
30. Cairns BR, Levinson RS, Yamamoto KR, Kornberg RD, Essential role of Swp73p in the function of yeast Swi/Snf complex. Genes Dev. 10, 2131 (1996). [PubMed: 8804308]
31. Kaeser MD, Aslanian A, Dong MQ, Yates JR 3rd, Emerson BM, BRD7, a novel PBAF-specific SWI/SNF subunit, is required for target gene activation and repression in embryonic stem cells. J Biol Chem283, 32254 (2008). [PubMed: 18809673]
32. Yan C, Chen H, Bai L, Systematic Study of Nucleosome-Displacing Factors in Budding Yeast. Mol. Cell71, 294 (2018). [PubMed: 30017582]
33. Lu YMet al., Dissecting the pet18 mutation in Saccharomyces cerevisiae: HTL1 encodes a 7-kDa polypeptide that interacts with components of the RSC complex. Mol. Genet. Genomics269, 321 (2003). [PubMed: 12684875]

34. Cairns BRet al., Two functionally distinct forms of the RSC nucleosome-remodeling complex, containing essential AT hook, BAH, and bromodomains. Mol. Cell4, 715 (1999). [PubMed: 10619019]

35. Yan L, Chen Z, A Unifying Mechanism of DNA Translocation Underlying Chromatin Remodeling. Trends Biochem. Sci (In press), (2019).

36. Harada BTet al., Stepwise nucleosome translocation by RSC remodeling complexes. Elife5, (2016).

37. Sabantsev A, Levendosky RF, Zhuang X, Bowman GD, Deindl S, Direct observation of coordinated DNA movements on the nucleosome during chromatin remodelling. Nat Commun10, 1720 (2019). [PubMed: 30979890]

38. Deindl Set al., ISWI remodelers slide nucleosomes with coordinated multi-base-pair entry steps and single-base-pair exit steps. Cell152, 442 (2013). [PubMed: 23374341]

39. Yen K, Vinayachandran V, Batta K, Koerber RT, Pugh BF, Genome-wide nucleosome specificity and directionality of chromatin remodelers. Cell149, 1461 (2012). [PubMed: 22726434]

40. Parnell TJ, Schlichter A, Wilson BG, Cairns BR, The chromatin remodelers RSC and ISW1 display functional and chromatin-based promoter antagonism. Elife4, e06073 (2015). [PubMed: 25821983]

. Dyer PNet al., Reconstitution of nucleosome core particles from recombinant histones and DNA. Methods Enzymol375, 23 (2004). [PubMed: 14870657]

. Clapier CR, Cairns BR, Regulation of ISWI involves inhibitory modules antagonized by nucleosomal epitopes. Nature492, 280 (2012). [PubMed: 23143334]

. Wittmeyer J, Saha A, Cairns B, DNA translocation and nucleosome remodeling assays by the RSC chromatin remodeling complex. Methods Enzymol377, 322 (2004). [PubMed: 14979035]

. Clapier CR, Langst G, Corona DF, Becker PB, Nightingale KP, Critical role for the histone H4 N terminus in nucleosome remodeling by ISWI. Mol. Cell Biol. 21, 875 (2001). [PubMed: 11154274]

. Punjani A, Rubinstein JL, Fleet DJ, Brubaker MA, cryoSPARC: algorithms for rapid unsupervised cryo-EM structure determination. Nat. Methods14, 290 (2017). [PubMed: 28165473]

. Zheng SQet al., MotionCor2: anisotropic correction of beam-induced motion for improved cryo-electron microscopy. Nat. Methods14, 331 (2017). [PubMed: 28250466]

. Rohou A, Grigorieff N, CTFFIND4: Fast and accurate defocus estimation from electron micrographs. J. Struct. Biol192, 216 (2015). [PubMed: 26278980]

. Scheres SH, Chen S, Prevention of overfitting in cryo-EM structure determination. Nat. Methods9, 853 (2012). [PubMed: 22842542]

. Bai XC, Rajendra E, Yang G, Shi Y, Scheres SH, Sampling the conformational space of the catalytic subunit of human gamma-secretase. Elife4, (2015).

. Pettersen EFet al., UCSF Chimera--a visualization system for exploratory research and analysis. J. Comput. Chem25, 1605 (2004). [PubMed: 15264254]

. Da Get al., Structure and function of the SWIRM domain, a conserved protein module found in chromatin regulatory complexes. Proc. Natl. Acad. Sci. U S A103, 2057 (2006). [PubMed: 16461455]

. Charlop-Powers Z, Zeng L, Zhang Q, Zhou MM, Structural insights into selective histone H3 recognition by the human Polybromo bromodomain 2. Cell Res. 20, 529 (2010). [PubMed: 20368734]

. Afonine PVet al., Towards automated crystallographic structure refinement with phenix.refine. Acta Crystallogr. D Biol. Crystallogr68, 352 (2012). [PubMed: 22505256]

. Liu F, Rijkers DT, Post H, Heck AJ, Proteome-wide profiling of protein assemblies by cross-linking mass spectrometry. Nat. Methods12, 1179 (2015). [PubMed: 26414014]

. Krzywinski Met al., Circos: an information aesthetic for comparative genomics. Genome Res. 19, 1639 (2009). [PubMed: 19541911]

. Funk Met al., Vector systems for heterologous expression of proteins in Saccharomyces cerevisiae. Methods Enzymol. 350, 248 (2002). [PubMed: 12073316]

. Chojnacki S, Cowley A, Lee J, Foix A, Lopez R, Programmatic access to bioinformatics tools from EMBL-EBI update: 2017. Nucleic Acids Res. 45, W550 (2017). [PubMed: 28431173]

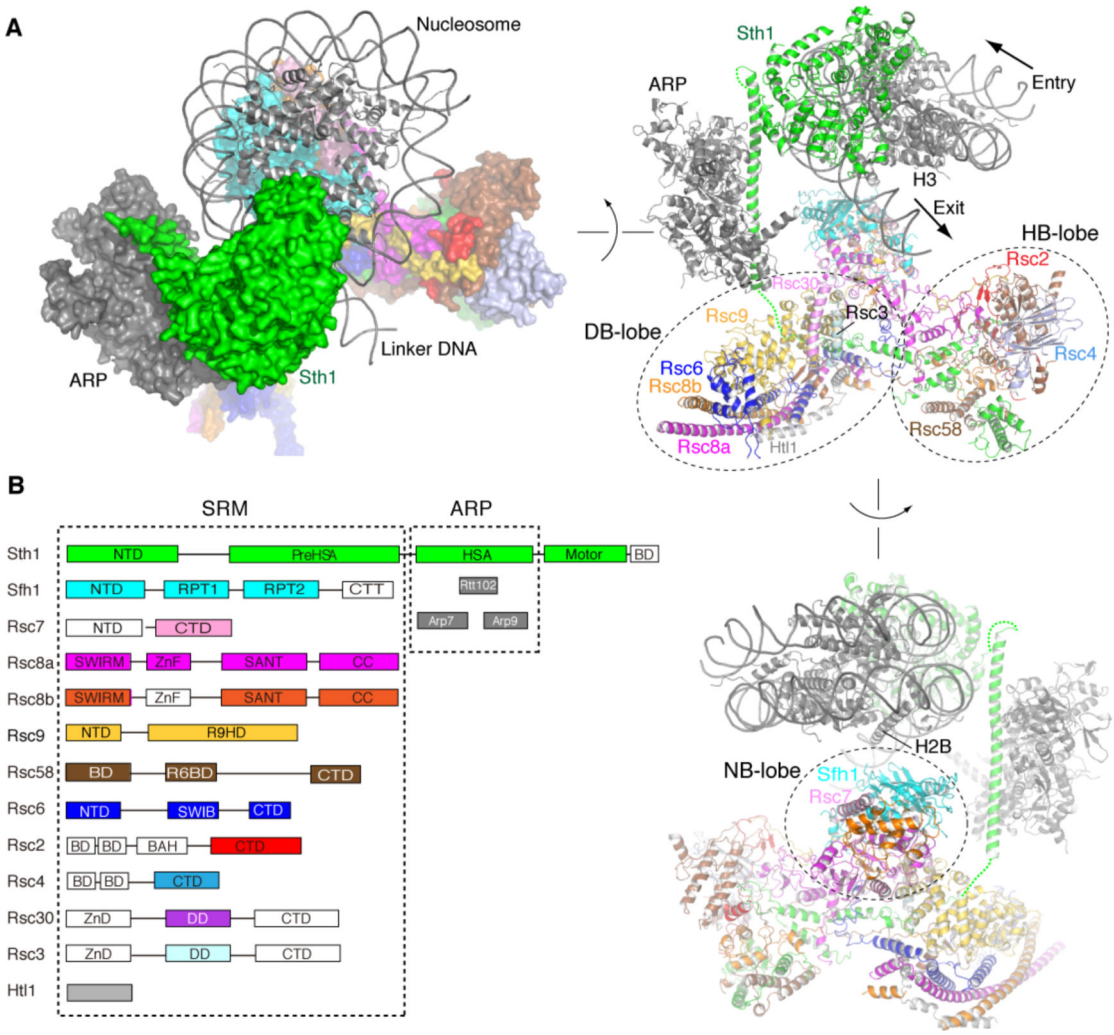

Figure 1. Overall structure of the RSC-nucleosome complex.

(**A**) Three different views of the structure of the complex. Arrows indicate the directionality of DNA translocation. (**B**) Domain architectures of the RSC subunits. The domains that are not structurally resolved in current study are colored white.

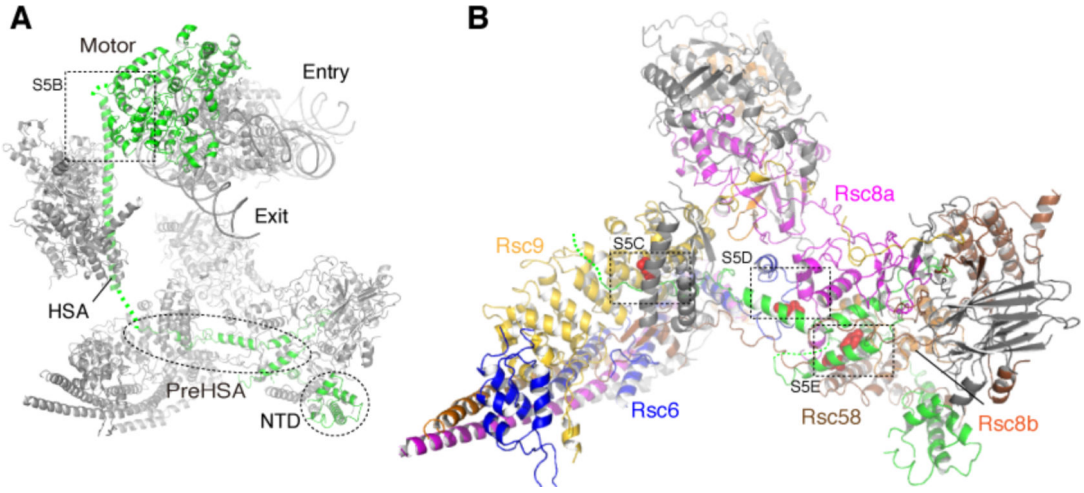

Figure 2. Structure of Sth1.

(**A**) Locations of the different domains of Sth1 within the RSC-nucleosome complex. The boxed region is enlarged in (Fig. S5B). (**B**) SRM assembly through preHSA. Residues related to the cancer-associated mutations in the human homologs are shown red spheres. The boxed regions are enlarged in Fig. S5C–S5E.

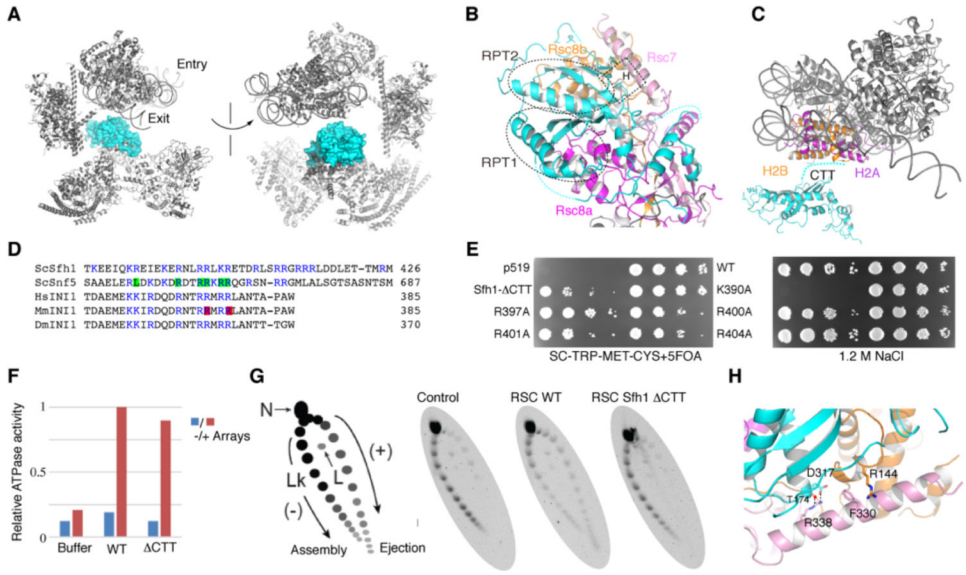

Figure 3. Structure of the NB-lobe.

(**A**) Sfh1 (cyan) is proximal to the nucleosome. (**B**) Structure of the NB-lobe. The boxed region is enlarged in (H). (**C**) The CTT of Sfh1 is close to the H2A (purple)-H2B (orange) surface. (**D**) Multiple sequence alignments of the CTTs of Sfh1-like proteins. The residues mutated in this study are highlighted in green. (**E**) Complementation assays of Sfh1 derivatives on synthetic dropout medium with FOA (left panel) and at high salt conditions (right panel). p519, control. (**F**) Relative ATPase activities of the WT and Sfh1-CTT RSC. (**G**) Comparative nucleosome ejection on plasmid arrays by WT and mutant RSC lacking the CTT. At left: schematic of the ejection assay, with supercoiled plasmid (topoisomer) distribution revealed by a 2D gel. Lk: Linking number, N: Nicked, L: Linear. A representative gel from multiple experiments is shown. (**H**) Interactions between Rsc7, Rsc8 and Sfh1.

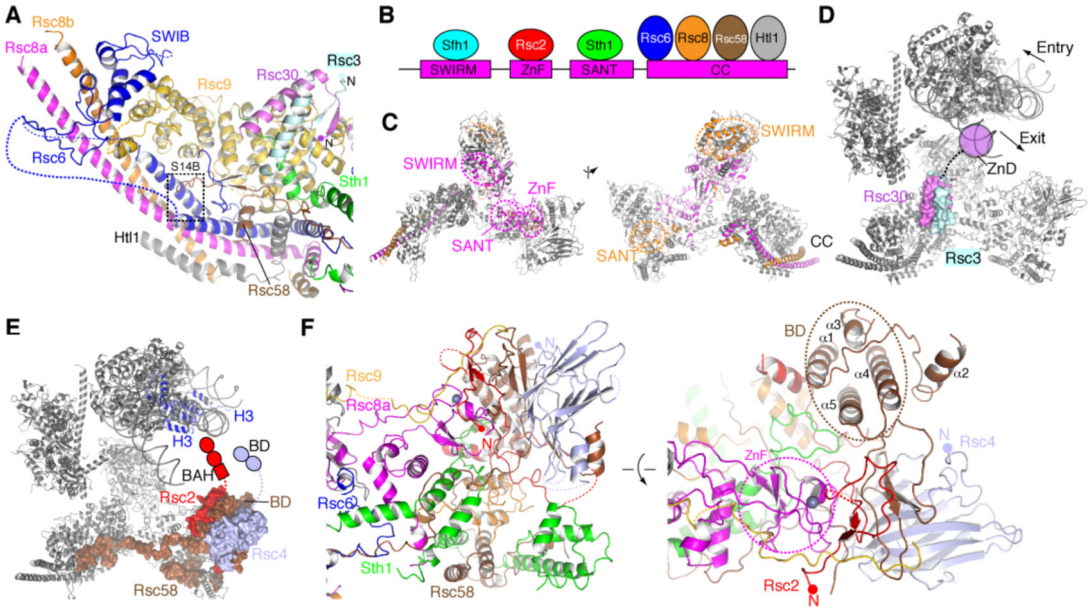

Figure 4. Structures of the DB-lobe and HB-lobe.

(**A**) Structure of the DB-lobe. The boxed region is enlarged for analysis in Fig. S14B. (**B**) Schematic illustration of the interactions of Rsc8 with other subunits of RSC. (**C**) Two different views of the Rsc8 structure. (**D**) Positions of Rsc3 and Rsc30. (**E**) Rsc2, Rsc4 and the BD of Rsc58 are located close to the N-terminal tails of histone H3. (**F**) Two different views of the structure of the HB-lobe.

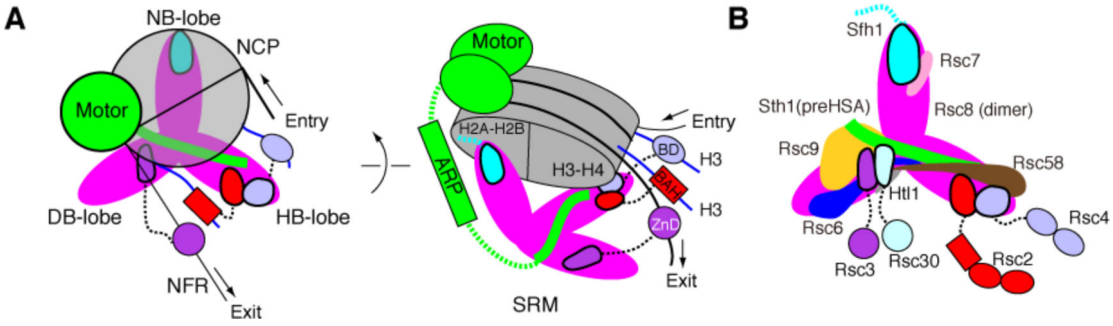

Figure 5. Model of the assembly and action of RSC

(**A**) Schematic of the structure of RSC bound to the nucleosome. Only the major structural elements are shown. DNA translocation results in the movement of the nucleosome away from the NFR. (**B**) Organization of the SRM.